p-ISSN 2089 – 0133 e-ISSN 2477-6416 Indonesian Journal of Applied Physics (IJAP) Vol. 12 No. 2 halaman 258
url : https://jurnal.uns.ac.id/ijap/article/view/60328 DOI : https://doi.org/10.13057/ijap.v12i2.60328

SIMULATION OF NEUTRON CONTAMINATION FROM MEDICAL LINAC USING PARTICLE AND HEAVY IONS TRANSPORT CODE SYSTEM (PHITS)

Bilalodin Bilalodin*, Aris Haryadi and Bejo Haryanto

Department of Physics, Faculty of Mathematics and Natural Sciences, Jenderal Soedirman University, Purwokerto, Indonesia
*corresponding author: bilalodin@unsoed.ac.id

Received 28-03-2022, Revised 25-06-2022, Accepted 12-09-2022
Available Online 04-10-2022, Published Regularly October 2022

ABSTRACT

Research on neutron contamination in medical LINAC has been carried out. The purpose of the study was to determine neutron contamination visually and to calculate the flux of neutron contamination produced by the LINAC device head. The research was conducted in a simulation using the Particle and Heavy Ion Transport code System (PHITS) . The LINAC model used in the simulation refers to the Siemens Primus LINAC head operating at voltages of 6 MV, 10 MV, 15, 18 MV, and 25 MV. The main components of the LINAC head model are the primary collimator, flattening filter, and secondary collimator. The radiation field area used is 10 x 10 cm^2 and the distance from the source to the surface of the water phantom object is 100 cm. The simulation shows that neutron contamination occurs due to photons' interaction with the LINAC components, namely the primary collimator, flattening filter, and secondary collimator. The operating voltages that produce neutron contaminants start at 10 MV. The increase in the voltage of the LINAC device causes a consequent increase in neutron flux. The calculation shows that the neutron flux on the surface of the water phantom is > 10^{11} n/cm^2.s Neutron flux has the potential to increase the total dose.

Keyword**:** Neutron contamination; Neutron flux; LINAC; PHITS

INTRODUCTION

A medical Linear accelerator (LINAC) is a high-voltage electron accelerator. The LINAC produces X-rays, which originate from the interaction of electrons with a target. A good target for producing X-rays comes from materials that have a high atomic number[1]. LINAC devices are widely used as radiotherapy equipment, especially for cancer or tumor therapy[2].

Treatment of tumors located deeper below the surface of the skin requires a LINAC with energy above 10 MeV. However, high energy LINAC devices will produce bremsstrahlung X-rays in addition to producing neutrons. Neutrons that are generated through the photoneutron mechanism are neutron contaminants, which are undesirable in therapy because it will increase the dose in a patient. The impact will be damage to healthy tissues[3].

Several studies have been conducted to understand the occurrence of neutron contaminants on LINAC devices. Martínez-Ovalle et al., (2011) studied the production of neutron contaminants in four different LINACs: Variant Clinac 2100 C, Elekta Inor, Elekta SL25, and Siemens Mevatron KDS, which operate at energies between 15 and 20 MV. The results

showed that the occurrence of neutron contaminants was strongly influenced by the type of target used on the LINAC device[4]. Further research was carried out by Nedaie et al., (2014) on the LINAC Varian 2100C device at a voltage of 18 MV. The simulation results show that the occurrence of neutron contaminants is highly dependent on the configuration of the LINAC[5]. Thekkedath et al., (2016) studied other effects that influence the occurrence of neutron contaminants on a LINAC device[6]. The results showed that the production of neutron contaminants is influenced by the radiation field area. Abu Talib et al., (2018) investigated the types of neutrons produced from the LINAC Elekta machine. The neutrons produced by LINAC are fast neutrons[7]. A recent study was conducted by Banaee et al., (2021) on the LINAC radiotherapy apparatus. The results showed that neutron contaminants occur due to the interaction of high energy photons > 8 MeV in materials that have high Z atoms[8].

Although several studies have been carried out to reveal the occurrence of neutron contamination, such research by displaying traces of neutron contaminants ranging from targets, collimators, and filtering filters to phantoms is still rare. The visualization will help explain the origin of the neutron contaminants. Consequently, pertinent efforts can be made to reduce neutron contaminants and avoid negative impacts on healthy tissue damage.

The traces of neutron contaminants can be visualized using the Particle and Heavy Ions Transport code System (PHITS). The PHITS is a nuclear simulation program issued by the Japan Atomic Energy Agency (JAEA). It uses nuclear data that combines the data banks of the Organization for Economic Co-operation and Development (OECD)/Nuclear Energy Agency (NEA), RSICC, and the Research Organization of Information and Technology (RIST). The PHITS program is suitable for simulating both charged and neutral particles. It is also equipped with a tally that can visualize particle traces in 2 dimensions and calculate physical quantity of interest[9]. In this work, we will describe the visualization results of the occurrence of neutron contaminants and calculate neutron flux using the PHITS code.

METHOD

LINAC Head Modeling

The medical LINAC model in the simulation is based on the Siemens Primus LINAC head model. The model used in the study consists of an electron source, a target, a primary collimator, a flattening filter, and a secondary collimator as the main components. The LINAC head components are made of Copper (Cu) target material. The primary and secondary collimator components are made of Tungsten (W), Nickel (Ni), and Iron (Fe), and the Flattening filter is made of copper (Cu)[10]. The model components of the LINAC head in two and three dimensions are shown in Figure 1.

The modeling of LINAC head components is simulated using the Particle and Heavy Ions Transport code System (PHITS) version 3.2 program. To get low statistical errors, the simulation is carried out with 10^6 particle history. The cross-sectional library data used for neutrons dan photons are JENDL-4.0, while for the electron is the intra-nuclear cascade (INCL4.6)[11]. The data is expected to guarantee the validity of the model.

The success in modeling the LINAC device will be demonstrated by the visualization of the x-ray photon trails generated by the interaction of the accelerated electrons with the target. In addition, the X-ray photon spectrum shows a spectrum of light energy consisting of characteristic X-rays and Bremsstrahlung[12,13].

Visualization and Calculation of Contaminant Neutron Flux

The visualization of the traces of contaminant neutron particles was carried out starting from the target to the surface of a water phantom which is $30 \times 30 \times 30$ cm^3 in size. The target distance from

the phantom surface is 100 cm. The collimator on the LINAC head is arranged so that the X-ray photons fall on a radiation field area of 10 x 10 cm^2 on the phantom surface[14]. To determine the occurrence of contaminant neutrons, the LINAC device is operated from voltages of 6, 8, 10, 15, 18, and 25 MV. Visualization of traces of neutron contamination and calculation of neutron flux was carried out by the PHITS program using tally tracks.

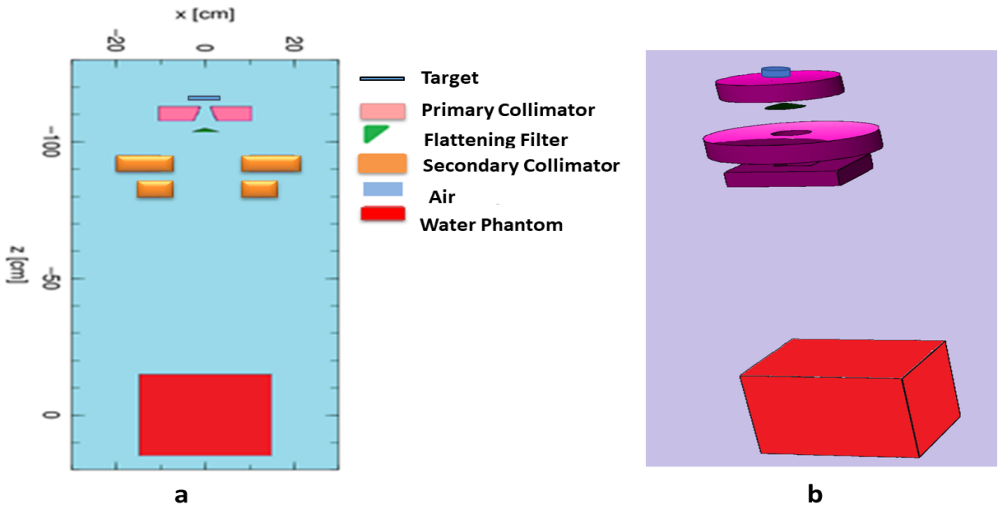

Figure 1. LINAC head and water phantom model (a) Two dimensions (c) Three dimensions

RESULTS AND DISCUSSION

LINAC Device-Head Modeling

The modeling has to be able to visualize the formation of the X-ray photon trace from the LINAC head and the X-ray spectrum. This is necessary to ensure that the designed model accords with the actual device[15]. According to the modeling, the X-ray photon trace produced by the LINAC head are shown in Figure 2a. The interaction of electrons with the target produces X-ray photons. The resulting photons scatter through the primary collimator, flatting filter, secondary collimator, and phantom. The highest photon flux intensity generated about the target is 10^{17} $p/cm^2.s$ (shown in red) and decreases further from the source and down to 10^{13} $p/cm^2.s$ (light blue) as it reaches the water phantom. The energy distribution of the resulting photons varies from 10^{-2} MeV to 6 MeV, forming a continuous curve. The continuous curve produced by the interaction of electrons with the target is called the Bremsstrahlung curve[16]. The resulting bremsstrahlung curve from the modeling is shown in Figure 2b.

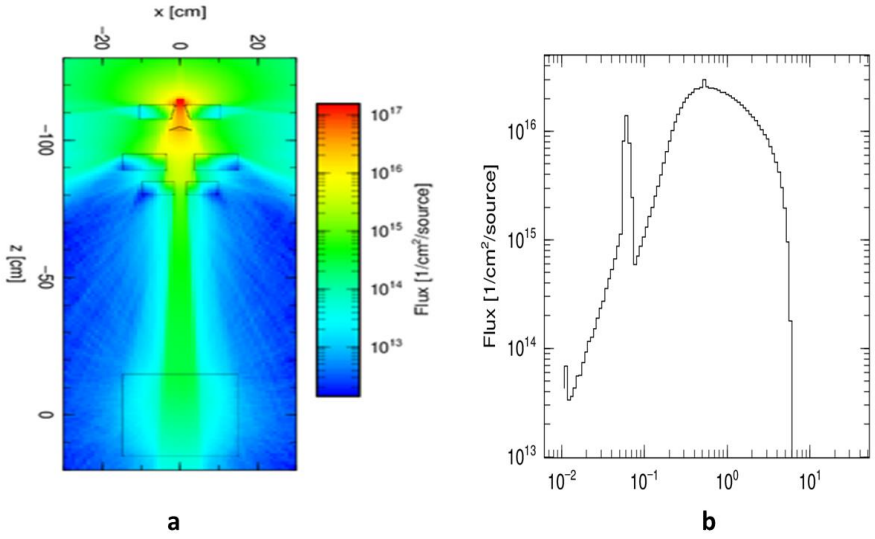

Figure 2. a. Simulation results of X-ray photon traces at 6 MV LINAC voltage. b. The energy spectrum of 6 MV X-ray

Neutron Contaminants

Figure 3 shows visualizations of neutron contaminants produced by the LINAC head components at operating voltages of (a) 6 MV, (b) 8 MV, (c) 10 MV, (d) 15 MV, (e) 18 MV, and (f) 25 MV. Neutron contaminants are depicted by color intensity. The highest intensity is shown in red, while the lowest intensity is shown in blue. The highest flux occurs around the primary collimator. The high intensity is generated by the primary collimator because this component is the first to interact with photons. The contribution of neutron contamination from the primary collimator in producing neutrons is about 55-60% of the total neutrons generated from the interaction of photons with LINAC head components[17]. Subsequently, the neutron intensity decreases after the photon interacts with the flattening filter and secondary collimator. Neutron contaminants produced by the components of LINAC head impinge on the water phantom at the voltages of 15, 18, and 25 MV.

The simulation results show that the interaction of X-ray photons with the components of the LINAC head material at a voltage of 6 MV with the target does not result in neutron contaminations. This is because at a voltage of 6 MV the X-ray photon energy is smaller than the threshold energy of the target[18]. (Threshold energy Cu= 9.91 MeV). As a result, no neutrons are released from the atomic nucleus during interactions. The intensity of neutron contaminants appeared and increased after the LINAC voltage reaches 8, 10, 15, 18, and 25 MeV. The increase in neutron contaminants is quite significant beyond the LINAC voltage of 15 MeV. At this voltage, the energy of the photons has exceeded the threshold energy of the primary collimator, flattening filter, and secondary collimator material. The primary collimator and secondary collimator are made from the same material. The threshold energy of the materials is W=6.74 MeV, Ni=7.63 MeV dan Fe 7.63 MeV. The threshold energy of the flattening filter made of Cu is 9.91 MeV[3].

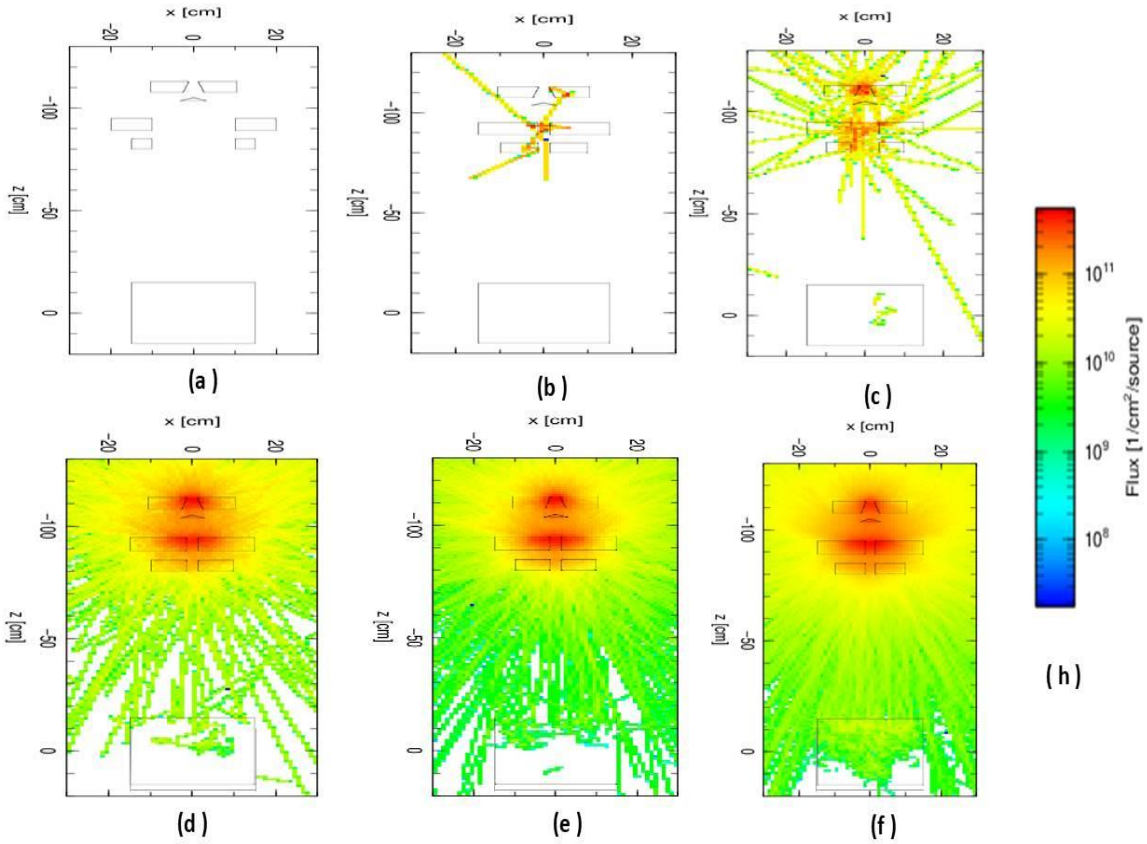

Figure 3. Visulalization of neutron contaminants produced by the components of the LINAC head at operating voltages of (a) 6 MV, (b) 8 MV, (c) 10 MV, (d) 15 MV, (e) 18 MV dan (f) 25 MV. (h) The conversion of intensity in the flux value of X-ray photon.

The spectrum of neutron contaminants is shown in Figure 4. The simulation results show that the spectrum of neutron contaminants is detected at voltages of 15, 18 and 25 MV. At a voltage of 15 MV the average energy of the neutron flux is at 0.23 MeV. Meanwhile, at 18 MV and 25 MV the average energy is at 0.35 MeV and 0.89 MeV. Neutrons are generated through a giant dipole resonance (GDR) reaction mechanism between photons and the LINAC head component [3]. Neutron contamination resulting from the interaction of X-ray photons with LINAC head components is in the form of fast neutrons. Fast neutrons have an energy range of 10^{-6} MeV to 10^{-2} MeV[15] .

The results of the simulation of visualization of neutron contamination using the PHITS program agree with the results of research conducted by Martínez-Ovalle et al., (2011), which states that the source of neutron contamination comes from the target [4]. The results of the study are also similar to those obtained by Nedaie et al., (2014) and Banaee et al, (2021), which state that the neutron source originates from the interaction of photons with the LINAC head components, especially interactions with materials with high Z[5,8]. The results also agree with the work of Abu Talib et al., (2018), which simulated LINAC with the MCNP program and found that the type of neutron contamination was fast neutrons[7].

The calculation results of the neutron flux on the surface of the water phantom at a voltage of 15 MV, 18 and 25 MV are, respectively, 1.82×10^{11} n/cm^2.s, 2.12×10^{11} n/cm^2.s, and 4.94×10^{11} n/ cm^2.s. Neutron flux impinging on the phantom can cause an increase in the total dose, which is the sum of the photon dose and the neutron dose[19,20,21]. The addition of

a neutron dose is formed through a fast neutron scattering mechanism with hydrogen atoms[22].

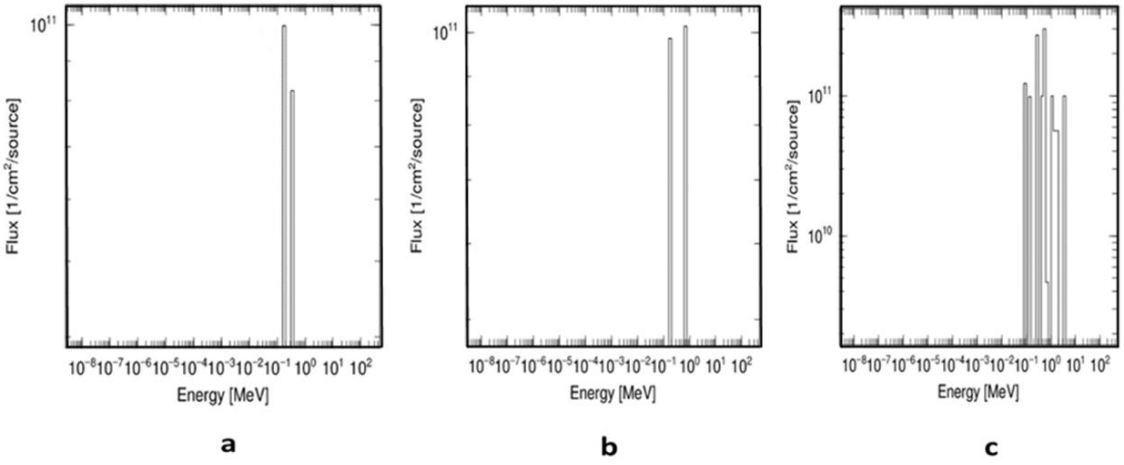

Figure 4. Spectrum of neutron contaminants at LINAC operating voltages of (a) 15 MV (b) 18 MV and (c) 25 MV

CONCLUSION

A simulation of the occurrence of neutron contamination from the medical LINAC has been carried out using the PHITS. The results of visualization neutron contamination using the PHITS show that neutron contaminants occurs due to the interaction of photons with the components of the LINAC head. Neutron contamination starts to appear at LINAC voltage of 10 MV and continues to increase as the LINAC voltage increases. This is so because, at this voltage, the photon energy produced by LINAC has exceeded the threshold energy limit of the neutron bond energy in the material that makes up the LINAC head. Neutron contamination resulting from the interaction of photons with LINAC head components is in the form of fast neutrons. The calculation result of neutron contaminants on the surface of the water phantom shows that the neutron flux reaches the surface of the water phantom at a LINAC voltage of 15, 18 dan 25 MV. The calculation results of the neutron flux on the surface of the water phantom at a voltage of 15 MV, 18 and 25 MV are, respectively, 1.82 $\times 10^{11}$ n/cm^2.s, 2.12 $\times 10^{11}$ n/cm^2.s, and 4.94 $\times 10^{11}$ n/ cm^2.s. Neutron flux has the potential to increase the total dose in a patient.

ACKNOWLEDGMENT

The author would like to thank the head of the computational and medical physics laboratory who has provided computer facilities. We also thank Mr. Anas as a computational and medical physics laboratory technician so that this research can be carried out.

REFERENCES

1. Quintieri, L., Bedogni, R., Buonomo, B., Esposito, A., De Giorgi, M., Mazzitelli, G., and Goméz-Ros, J. M. 2012. Photoneutron Source by High Energy Electrons on High Z Target: Comparison between Monte Carlo Codes and Experimental Data. *Fusion Science and Technology*, 61(1T), 314-321.
2. Hao, J., Magnelli, A., Godley, A., and Jennifer, S. Y. 2019. Use of a Linear Accelerator for Conducting In Vitro Radiobiology Experiments. *JoVE (Journal of Visualized Experiments)*, 147, e59514.

3. Naseri, A., and Mesbahi, A. 2010. A review on photoneutrons characteristics in radiation therapy with high-energy photon beams. *Reports of practical oncology and radiotherapy*, *15*(5), 138-144.
4. Martinez-Ovalle, S. A., Barquero, R., Gomez-Ros, J. M., and Lallena, A. M. 2011. Neutron dose equivalent and neutron spectra in tissue for clinical linacs operating at 15, 18 and 20 MV. *Radiation protection dosimetry*, 147(4), 498-511.
5. Nedaie, H. A., Darestani, H., Banaee, N., Shagholi, N., Mohammadi, K., Shahvar, A., and Bayat, E. 2014. Neutron dose measurements of Varian and Elekta linacs by TLD600 and TLD700 dosimeters and comparison with MCNP calculations. *Journal of medical physics/Association of Medical Physicists of India*, 39(1), 10.
6. Thekkedath, S. C., Raman, R. G., Musthafa, M. M., Bakshi, A. K., Pal, R., Dawn, S., and Datta, D. 2016. Study on the measurement of photo-neutron for15 MV photon beam from medical linear accelerator under different irradiation geometries using passive detectors. *Journal of Cancer Research and Therapeutics*, 12(2), 1060.
7. Abou-Taleb, W. M., Hassan, M. H., El_Mallah, E. A., and Kotb, S. M. 2018. MCNP5 evaluation of photoneutron production from the Alexandria University 15 MV Elekta Precise medical LINAC. *Applied Radiation and Isotopes*, 135, 184-191.
8. Banaee, N., Goodarzi, K., and Nedaie, H. A. 2021. Neutron contamination in radiotherapy processes: a review study. *Journal of Radiation Research*, 62(6), 947-954.
9. Hashimoto, S., Iwamoto, O., Iwamoto, Y., Sato, T., and Niita, K. 2015. PHITS simulation of quasi-monoenergetic neutron sources from 7Li (p, n) reactions. *Energy Procedia*, 71, 191-196.
10 Abou-Taleb, W. M., Hassan, M. H., El_Mallah, E. A., and Kotb, S. M. 2018. MCNP5 evaluation of photoneutron production from the Alexandria University 15 MV Elekta Precise medical LINAC. *Applied Radiation and Isotopes*, *135*, 184-191.
11. Sato, T., Niita, K., Matsuda, N., Hashimoto, S., Iwamoto, Y., Furuta, T., and Sihver, L. 2013. Overview of particle and heavy ion transport code system PHITS. *Annals of Nuclear Energy*, 82, 110-11
12. Ezzati, A. O., Studenski, M. T., and Gohari, M. 2020. Spatial mesh-based surface source model for the electron contamination of an 18 MV photon beams. *Journal of medical physics*, 45(4), 221.
13. Almatani, T. 2021). Validation of a 10 MV photon beam Elekta Synergy linear accelerator using the BEAMnrc MC code. *Journal of King Saud University-Science*, 33(4), 101406
14. Amour, K., Maleka, P., Maunda, K., Mazunga, M., and Msaki, P. 2020. Verification of Depth Dose Curves Derived on Beeswax, Paraffin and Water Phantoms Using FLUKA Monte Carlo Code. *Tanzania Journal of Science*, 46(3), 923-930.
15. Jabbari, I., and Monadi, S. 2015. Development and validation of MCNPX-based Monte Carlo treatment plan verification system. *Journal of medical physics/Association of Medical Physicists of India*, 40(2), 80.
16. Bilalodin, B., Suparta, G. B., Hermanto, A., Palupi, D. S., Sardjono, Y., and Rasito, R. 2020. Analysis of particle distribution in a double layer beam shaping assembly resulted from 30 MeV-proton reactions with beryllium target using the PHITS program. *Jurnal Teknologi*, 82(3).
17. Dawn, S., Pal, R., Bakshi, A. K., Kinhikar, R. A., Joshi, K., Jamema, S. V., and Datta, D. 2018. Evaluation of in-field neutron production for medical LINACs with and without flattening filter for various beam parameters-Experiment and Monte Carlo simulation. *Radiation Measurements*, 118, 98-107
18. Patil, B. J., Chavan, S. T., Pethe, S. N., Krishnan, R., Bhoraskar, V. N., and Dhole, S. D. 2010. Simulation of e–γ–n targets by FLUKA and measurement of neutron flux at various angles for accelerator based neutron source. *Annals of Nuclear Energy*, 37(10), 1369-1377.
19. Khaledi, N., Dabaghi, M., Sardari, D., Samiei, F., Ahmadabad, F. G., Jahanfarnia, G., and Wang, X. 2018. Investigation of photoneutron production by Siemens artiste linac: A Monte Carlo Study. *Radiation Physics and Chemistry*, 153, 98-103.
20 Tai, D. T., Loan, T. T. H., Sulieman, A., Tamam, N., Omer, H., and Bradley, D. A. 2021. Measurement of Neutron Dose Equivalent within and Outside of a LINAC Treatment Vault Using a Neutron Survey Meter. *Quantum Beam Science*, 5(4), 33.

21. Dowlatabadi, H., Mowlavi, A. A., Ghorbani, M., Mohammadi, S., and Knaup, C. 2020. Study of photoneutron production for the 18 mv photon beam of the siemens medical linac by monte carlo simulation. *Journal of Biomedical Physics & Engineering*, 10(6), 679.
22. Shahmohammadi Beni, M., Hau, T. C., Krstic, D., Nikezic, D., and Yu, K. N. 2017. Monte Carlo studies on neutron interactions in radiobiological experiments. *PLoS One*, *12*(7), e0181281